COMPDYN 2013
4th ECCOMAS Thematic Conference on
Computational Methods in Structural Dynamics and Earthquake Engineering
M. Papadrakakis, N.D.Lagaros, V. Plevris (eds.)
Kos Island, Greece, 12–14 June 2013

Effect of Spatially Variable Ground Motions on the Seismic Fragility of Box Girder Continuous Bridges

H.A. Elhowary[1], O. Ramadan[2], S.S.F. Mehanny[3]

[1]Bridge Design Engineer, Dar Al-Handasah, Giza, Egypt
Ph.D. Graduate student, Cairo University, Egypt
Hesham.Ayman2010@gmail.com

[2]Professor of Structural Engineering, Faculty of Engineering, Cairo University, Giza, Egypt
omoramadan@yahoo.ca

[3]Professor of Structural Engineering, Faculty of Engineering, Cairo University, Giza, Egypt
sameh.mehanny@stanfordalumni.org

Keywords: Spatially variable ground motions, Seismic Fragility, Box Girder Continuous bridges

Abstract. *Seismic design of bridges is usually performed assuming that all bridge supports experience the same ground motion (i.e. uniform input). However, strong-motion recorders of special seismograph arrays already demonstrated that significant spatial variation do exist in seismic ground motions [1]. The spatial variation of seismic ground motions is due to various sources including the loss of coherency, which results from random reflections and refractions as the waves travel through the soil, and the wave-passage effect.*

The present paper illustrates the impact of ground motion spatial variability on the seismic performance of continuous box girder bridges in both bridge orthogonal directions (longitudinal and transverse). For illustration purposes, a nine-span bridge with a total length of 430m is adopted. Non-linear time history analyses are carried out using OPENSEES software [2]. The wave passage effects are examined individually using a set of real records originally extracted from the PEER (Pacific Earthquake Engineering Center) Strong Motion Database using different apparent wave propagation velocities. Then, the loss of coherency effect is investigated using a set of artificially simulated seismic ground motions using the SIM software developed by Ramadan and Novak [3& 4] considering different degrees of loss in coherency and various ground motion frequency contents.

Results of the non-linear time history analyses performed in an incremental dynamic analysis context are hence manipulated through a probabilistic analysis framework to generate fragility curves associated with various performance levels for the case study bridge. Fragility curves giving the conditional probability of exceeding various performance levels are then integrated with generated hazard curves defining the expected seismic hazard in Egypt. The outcome of this integration process results in values of mean annual frequency of exceeding pre-defined performance levels.

1 INTRODUCTION

In the current seismic-resistant design of structures, the seismic ground motion excitations at their supports are assumed to be identical (i.e. uniform excitation for a given structure). However, for extended lifeline systems, the implementation of identical motions at the supports of these extended structures can yield un-conservative structural responses. Therefore, spatially variable seismic ground motions should be considered in their seismic response analysis and design. Since the 1960s, the effects of seismic ground motion spatial variation on lifeline structures have been studied. The results indicate that the type of response (conservative or un-conservative) induced by the spatially variable motions compared to that of identical ones depends strongly on the spatial variation models used in the analysis, and a realistic characterization of seismic ground motion spatial variation is highly desired. It is hence further realized that spatially variable seismic ground motions reflect the true motions at the supports of a given bridge [5].

The present paper studies the effect of spatially variable ground motions on the seismic response of continuous concrete highway bridges. Finite element models of a case study bridge are hence created for the non-linear incremental dynamic time history analyses. Linear models are developed for design purposes using SAP2000, while nonlinear analyses are carried out using OPENSEES (Open System for Earthquake Engineering and Simulation). After designing the case study bridge, displacement controlled non-linear pushover analyses are carried out using OPENSEES software. Displacement controlled non-linear pushover analyses in both bridge orthogonal directions are performed prior to the non-linear time history analyses in order to quantify the resistance of the bridge to the lateral deformation and to gauge the mode of deformation. Pushover analyses are carried out by applying gravity loads to the bridge deck and then applying incremental displacement at the deck level up to values corresponding to various performance levels until reaching collapse. Drift values/limits associated with various performance levels are hence identified.

The spatial variation in seismic ground motions has three main sources summarized as follows: firstly is the wave passage effect resulting from the difference in the arrival time of the seismic waves at different locations within the structure; secondly is the incoherence effect resulting from the differences in the manner and the method of the superposition of seismic waves due to the arrival from an extended source and scattered irregularities and in-homogeneities along the path and at the site; and finally is the "Local" site effects due to the differences in the local soil conditions at each support which may alter the frequency content and amplitude of the bedrock motions.

While studying the wave passage effects the parametric analyses are carried out using five actual time history records with different apparent propagation velocities (100m/sec, 200m/sec, 400m/sec and v=Infinity which is equivalent to the uniform excitation scenario) of the seismic waves. The five records pertain to the large database of records gathered in Medina (2002) [6] and are originally extracted from the PEER (Pacific Earthquake Engineering Center) strong motion database (PEER Strong Motion Catalog). The ground motions represented by the records are characteristic of the non-near-fault motions recorded in California.

On the other hand, when studying the loss of coherency effects on the seismic performance of the case study bridge, various sets of artificially simulated ground motions have been adopted. These sets of the seismic ground motions are generated using the SIM software developed by Ramadan and Novak [3&4] considering various levels of loss in coherency (c/v=0.0001, 0.001, 0.002) in addition to c/v=zero representing the fully coherent seismic waves. In addition to the different loss of coherency degrees, three response spectra representing various soil types are examined.

Performed fragility analyses consider various types of uncertainties: demand uncertainty ($\beta_{D|Sa}$), capacity uncertainty (β_{CL}), and modeling uncertainty (β_M). Different levels of uncertainties in both capacity and modeling are examined and the influence of such uncertainties on altering the results is also presented. Modeling of uncertainties is performed as per Taylor (2007) [7].

2 DESCRIPTION OF THE CASE STUDY BRIDGE

The selected case study bridge is a 9-span bridge with a total length of 430m (40+7×50+40) as shown in figure 1. The two central piers are monolithic with the deck while their adjacent piers (one pier at each side of the monolithic piers) are equipped with fixed pot bearings. In addition, guided bearings allowing translation of the deck in the longitudinal direction are adopted at all other piers and at abutments in order to release all thermal effects away from the central restrained part.

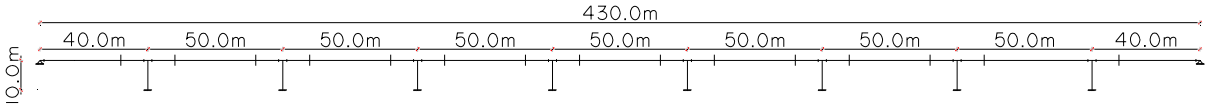

Figure 1: Layout and span arrangement of the case study bridge

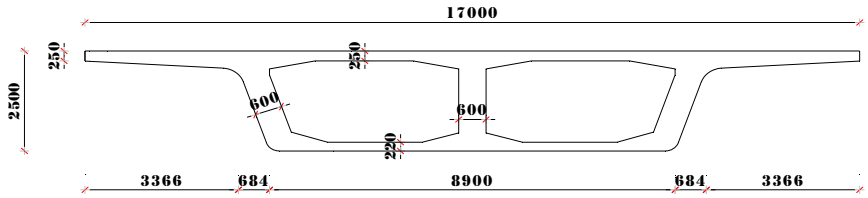

Figure 2: Typical section for the case study bridge (Dimensions in mm)

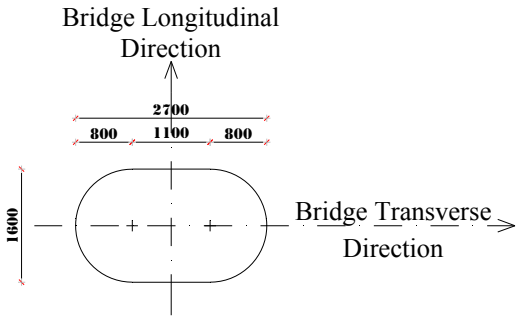

Figure 3: Typical pier section (Dimensions in mm)

The bridge deck is a post-tensioned double vent box section with a typical section as shown in figure 2. It has a constant depth of 2.5m (Span/Depth=20) and total width of 17.0m while the bridge piers are reinforced concrete piers with typical dimensions of 1.6m x 2.7m and a constant height of 10m as shown in figures 1 and 3.

The case study bridge is designed to sustain gravity loads according to [8] (ECP 201-2008 - Egyptian code for determination of loads and forces in the structural and civil works). Gravity loads include dead and super-imposed dead loads in addition to the highway live loads and pedestrian live loads. Seismic design loads are also in accordance with (ECP 201-2008) based on zone 5A. In this seismic zone, bridges shall be designed to withstand expected seismic loads resulting from a peak ground acceleration of 0.25g. This value of 0.25g as a peak ground acceleration represents nearly the highest seismic hazard in Egypt, while it corresponds to a medium seismic hazard in California USA. The seismic design is performed by the multi-modal response spectrum method as per clause 9.5 and Table 9-2 of ECP 201-2008 [8].

Type (1) response spectrum for Soil type B is adopted for the bridge seismic design. Type (1) spectrum is used for all regions in Egypt except coastal regions on the Mediterranean Sea (within 40 km alongside the coastline). In addition to the above stated seismic design criteria, the response modification factor (force reduction factor) "R" is taken equal to 5. This value corresponds to the use of reinforced concrete piers with sufficient ductility and relevant reinforcement details enabling the formation of a plastic hinge mechanism as per Table 9-3 of ECP 201-2008.

3 PUSHOVER ANALYSES AND MONITORED DAMAGE INDICES

3.1 Pushover analyses for the case study bridge in longitudinal and transverse directions

Displacement-controlled pushover analyses are conducted herein on the OPENSEES baseline models for the case study bridge. Pushover analysis consists of first applying the distributed gravity load to the bridge and then applying incremental displacements at the deck level until reaching a given target displacement. The main advantage of carrying the pushover analysis as widely presented in the literature is to determine the lateral load capacity of the bridge by plotting the relation between the base shear and the deck drift; or by plotting the percentage of the design base shear versus the deck drift of the bridge. This percentage, when above 100%, simply defines the so-called static over-strength of the bridge as-designed. The relation between the percentages of design base shear and the deck drift for the bridge in both directions is given below in figures 4a and 4b.

Referring to figures 4a and 4b, the collapse limit state for the case study bridge performing non-linear pushover analysis in the longitudinal direction is captured at a deck drift ratio of 2.55% (δ_θ =2.55 %). This collapse is assumed at 20% loss in the piers section capacity. Such result is in close agreement with previous research work in the literature as presented in table 2. On the other hand, performing the non-linear pushover analysis in the transverse direction results in different deck drift values corresponding to the same damage limit states monitored for the longitudinal direction. For instance, the collapse limit state in the transverse direction is captured at a deck drift ratio equal to 4.60% (δ_θ =4.60 %). This difference is due to the following

main factors affecting the transverse direction relative to the longitudinal direction: firstly, the end conditions for the pier in the longitudinal direction are different from those in the transverse direction. Secondly, the inertia and the section moment capacity/strength of the piers in the transverse direction are larger than those in the longitudinal direction (usually 5 to 10 folds in the majority of bridges). Moreover, the number of piers resisting the transverse seismic loads is larger than the number of piers resisting the longitudinal loads due to the adopted bearings articulation. In other words, it is common practice to adopt larger number of bearings guided (i.e., allowing translation) in the longitudinal direction to minimize the thermal effects; to the contrary all these bearings are restrained in the transverse direction. Finally is the deformed shape of the bridge deck under the effect of the horizontal monotonic loads (or under seismic loads) in the transverse direction which totally differs from that in the longitudinal direction due to the absence of the framing action that exists in the longitudinal direction.

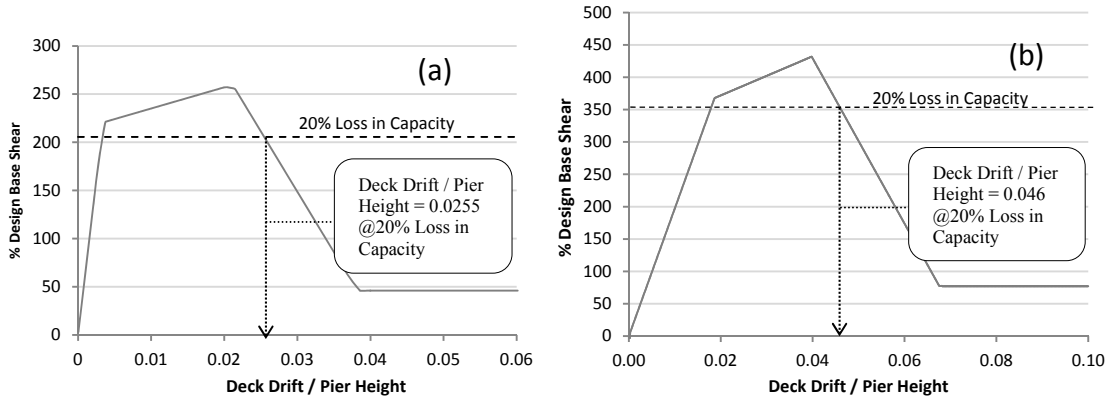

Figures 4: Deck drift ratios versus % of design base shear for the bridge longitudinal direction (figure a) and the transverse direction (figure b)

Due to all above mentioned factors, higher values for deck drift capacity in the transverse direction relative to these in the longitudinal direction are observed for the same damage limit states.

Table 1: Summary of the pushover analysis results for the case study bridge

Loading Direction	**Capacity as % Design Base Shear (Static Over-strength x 100)**	**Deck Drift/ Pier Height @ 20% loss in capacity**	**$R_{eff.}$**
Longitudinal	257	0.0255	2.20
Transverse	430	0.0460	3.70

Table 1 also presents another format of the over-strength values ($R_{effective}$) that is calculated according to [9] as follows:

$$R_{effective} = \frac{S_a(T_1)\,|_{\text{Elastic code response spectrum (R=1)}}}{S_{ay}} \qquad (1)$$

Where, S_{ay} is the yield spectral acceleration and may be computed as $F_y/(W/g)$. F_y is the yield base shear (i.e., the base shear at the end of the first linear part of the "base shear-deck drift" curve).

3.2 Monitored damage indices

For a given S_a (T1) for a specific bridge the time history inelastic analyses are carried out as outlined in sections 4 and 5 and different potential damage indices (or, damage measures) are monitored. The different damage indices monitored herein are as follows:

A- Maximum deck drift which is a pre-defined value corresponding to a certain performance level or even to collapse level. The deck drift value at a certain excitation level in the longitudinal direction is only one value for the whole deck as the deck is acting as a rigid diaphragm in the longitudinal direction. However, under transverse direction excitation the deck drift referred to herein is corresponding to the maximum drift value occurring in the deck. Table 2 presents the different deck drift limits in accordance with the corresponding values extracted from the pushover analyses presented in section 3.1.

Table 2: Deck drift damage limit states as previously defined in SEAOC [10] for the longitudinal and transverse directions

Damage Scale Definition (Limit States)	**Damage description**	**Deck Drift (δ_θ %)**	
		Longitudinal Direction	**Transverse Direction**
Fully Operational	Negligible	**<0.2**	**<0.5**
Operational	Minor local yielding at some piers may occur. No observable fractures. Minor buckling or observable permanent distortion of the bridge members.	**0.2 to 0.5**	**0.5 to 1.0**
Life safety	Hinges form. Local buckling of some elements. Severe joint distortion. Isolated connection failures. A few elements may experience fracture.	**0.5 to 1.5**	**1.0 to 3.5**
Near Collapse	Extensive distortion for the structure components and pier panels. Many fractures in connections.	**1.5 to 2.5**	**3.5 to 5.0**
Complete Collapse	-	**> 2.5**	**> 5.0**

It is worth reporting that complete collapse has been captured in the present research at deck drift ratios very close to values shown in table 2 gathered from the literature [10]. Collapse is defined herein at 20% loss in the base shear capacity as previously proposed in the literature.

B- Maximum pier rotation (considered a direct measure of both global and local damage of the bridge) at a certain performance level. Performance levels can be directly correlated to the piers rotation values as follows: (a) yield performance level, (b) post yield performance level which corresponds to the isotropic hardening rotation of the piers and (c) ultimate rotation which corresponds to the collapse level where the rotation of the pier section is uncontrolled.

C- Shear failure in the bridge piers.

D- Unseating of the deck at the piers where the deck is supported by guided sliding bearings.

E- Excessive deck compressive or tensile stresses which may result in the failure of the deck pre-stressing system.

Note that due to space limitations only results considering the deck drift damage index are presented herein. However, other damage indices are investigated and presented in [11], but they are found to be non-controlling from design/performance perspective when compared to the deck drift.

4 WAVE PASSAGE EFFECT ON CASE STUDY BRIDGE

Wave passage effect results from the difference in the arrival times of seismic waves at different locations along the bridge. The influences of the wave-passage effect on the responses of bridges have been investigated by several researchers. However, most of these studies focus on the elastic behavior of the structure with very few of those studies dealing with the nonlinear responses of bridges. Monti et al. [12] studied the nonlinear responses of symmetric bridges with symmetric boundary conditions. They have found that the travelling wave effect on the response results essentially in a reduction of the dynamic part due to the incomplete synchronization of the excitation for the range of apparent velocities in excess of 500 m/s. Tzanetos et al. [13] studied the wave-passage effect on the inelastic responses of symmetric bridges with symmetric or asymmetric boundary conditions. They concluded that special consideration should be given to bridges with asymmetric boundary conditions since they may respond in higher modes more readily than symmetric structures and the demands are likely to increase on those bridges. However, their studies adopted simplified structural models.

In this research work, a study of the inelastic seismic responses of the case study bridge is carried out in both longitudinal and transverse directions using the OPENSEES software. Parametric analyses using five different time history records with different propagation velocities of the seismic waves are conducted to assess the wave-passage effect on the response of the bridge. The response of the bridge to asynchronous input motions at different pier bases consists of two components [14]: a dynamic component induced by the inertia forces and a so-called pseudo-static component, due to the difference between the adjacent support displacements. It is observed that the propagation velocity of seismic waves has a significant effect on the response of the bridge. When the travelling apparent wave velocity is lower than 150 ~ 250m/s, the response is dominated by the pseudo-static component. As the travelling wave velocity increases, the pseudo-static component is considerably reduced and the dynamic component increases rapidly. When the travelling wave velocity is higher than 150~250m/s, the response is dominated by the dynamic component, Wang et al. [15].

4.1 Ground motions selected for the wave passage effect analyses

A bin of 5 ground motions is selected for the present time history analysis in the context of the fragility/vulnerability seismic assessment of case study bridges presented in this research work. The 5 records pertain to the large database of records gathered in Medina [6] and are originally extracted from PEER Strong Motion Catalog. The ground motions represented by the records are characteristic of non-near-

fault motions recorded in California; details of the adopted 5 records are presented in table 3.

Table 3: Summary of the earthquake records used in wave passage effect analyses

Record ID	Event	Year	Mw	Station	R (km)	Mechanism	f_{HP} (Hz)	PGA (g)	PGV (cm/s)	PGD (cm)	Duration Length (sec)
IV79dlt	Imperial Valley	1979	6.5	Delta	43.6	strike-slip	0.05	0.24	26.0	12.10	99.90
CO83c05	Coalinga	1983	6.4	Parkfield-Cholame 5W	47.3	reverse-oblique	0.20	0.13	10.0	1.30	40.00
IV79cc4	Imperial Valley	1979	6.5	Coachella Canal #4	49.3	strike-slip	0.20	0.13	15.6	3.00	28.50
IV79cmp	Imperial Valley	1979	6.5	Compuertas	32.6	strike-slip	0.20	0.19	13.9	2.90	36.00
WN87bir	Whittier Narrows	1987	6	Downey-Birchdale	56.8	reverse	0.15	0.30	37.8	5.00	28.60

where,

M_w = Earthquake Magnitude,
R = Fault rupture distance,
F_{HP} = High-pass frequency,
and $f_{HP} \leq 0.2$

4.2 Results of the wave passage effect analyses in bridge longitudinal and transverse directions

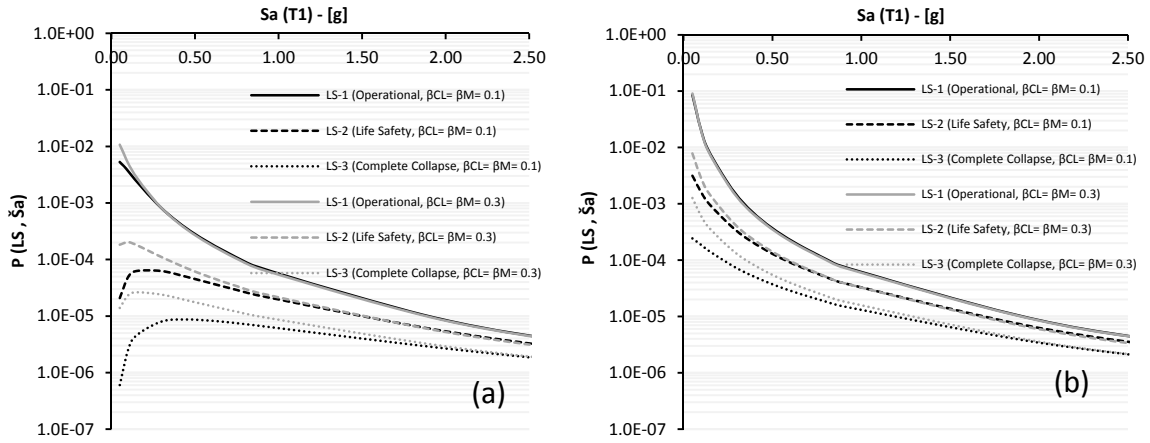

Figure 5: Joint probability curves of exceeding various performance levels versus S_a levels at different levels of uncertainty in capacity and modeling in the bridge longitudinal direction at v =100m/sec (figure a) and v =Infinity (figure b) (Log-scale)

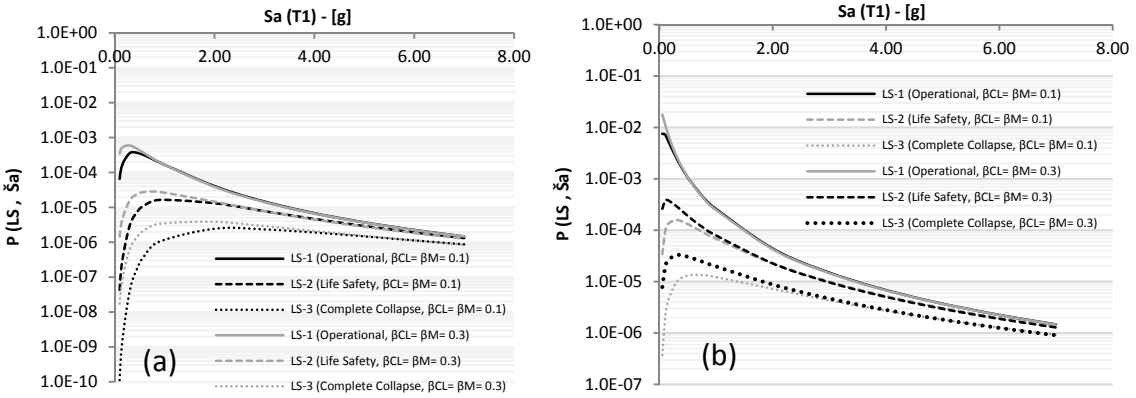

Figure 6: Joint probability curves of exceeding various performance levels versus S_a levels at different levels of uncertainty in capacity and modeling in the bridge transverse direction at v =100m/sec (figure a) and v =Infinity (figure b) (Log-scale)

Figures 5 and 6 represent samples of the joint probability curves of exceeding various performance levels versus S_a levels considering different levels of uncertainties in demand, capacity and modeling.

The "joint" probability equals the probability of exceeding a certain limit state (conditional probability) integrated over the whole expected hazard (shown in figure 7) during the life time of the structure. For detailed information refer to El-Howary (2014) [11]. Referring to the sample figures 5 and 6, one could notice that considering the uncertainties in demand, modeling and capacity may alter the results and adversely affect (i.e., underestimate) the capacity of the structure by a considerable amount. In other words, considering uncertainties may increase the probability of reaching pre-defined performance levels or reaching collapse.

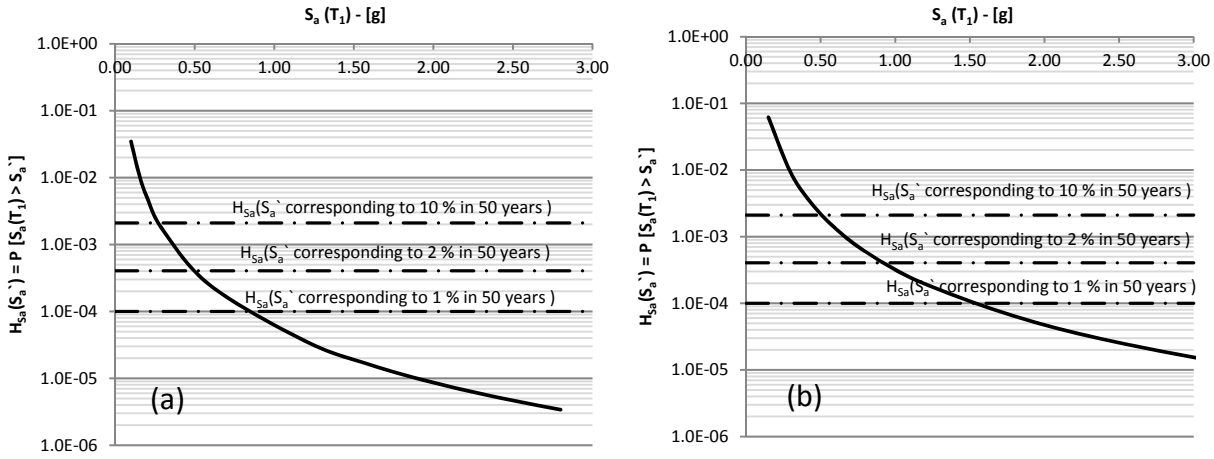

Figure 7: Annual hazard curves for case study bridge (5 % Damping – Soil class B) in the longitudinal direction (figure a) and in the Transverse direction (figure b) - El-Howary (2014) [11]

The hazard curves shown in figure 7 are generated following the same approach as in previous research work which adopts similar hazard curves in the probabilistic seismic assessment of RC moment frame buildings in Egypt [16].

The mean annual frequency of exceeding the target performance levels at different selected levels of uncertainties is illustrated in table 4. Reported results in table 4 are given for some apparent wave propagation velocities investigated in the present research.

Table 4: Mean Annual Frequency of exceeding various performance levels for the case study bridge in longitudinal and transverse directions

Limit State*	Apparent Wave propagation Velocity (m/sec)	λ (MAF of exceeding target performance levels)					
		Longitudinal Direction			Transverse Direction		
		$\beta_{CL}=\beta_M=0.1$	$\beta_{CL}=\beta_M=0.2$	$\beta_{CL}=\beta_M=0.3$	$\beta_{CL}=\beta_M=0.1$	$\beta_{CL}=\beta_M=0.2$	$\beta_{CL}=\beta_M=0.3$
LS-1	100	1.29E-02	1.57E-02	2.01E-02	1.80E-03	2.16E-03	2.93E-03
	200	6.66E-02	7.11E-02	7.71E-02	2.51E-02	3.05E-02	4.04E-02
	400	9.41E-02	9.74E-02	1.02E-01	2.58E-02	3.16E-02	4.22E-02
	∞	1.15E-01	1.17E-01	1.20E-01	2.37E-02	2.94E-02	3.97E-02
LS -2	100	3.43E-04	4.95E-04	8.63E-04	8.85E-05	1.14E-04	1.67E-04
	200	2.39E-03	3.50E-03	5.70E-03	9.64E-04	1.28E-03	2.00E-03
	400	4.31E-03	6.08E-03	9.37E-03	8.99E-04	1.21E-03	1.94E-03
	∞	6.37E-03	8.73E-03	1.29E-02	7.65E-04	1.05E-03	1.72E-03
LS -3	100	5.26E-05	7.89E-05	1.49E-04	1.28E-05	1.61E-05	2.39E-05
	200	2.77E-04	4.75E-04	9.89E-04	1.03E-04	1.42E-04	2.35E-04
	400	4.98E-04	8.56E-04	1.73E-03	8.96E-05	1.26E-04	2.15E-04
	∞	7.58E-04	1.28E-03	2.51E-03	7.18E-05	1.03E-04	1.80E-04

* LS-1=Operational Limit state, LS-2=Life safety and LS-3=Complete Collapse (Refer to table 2 for limit states description)

As shown in table 4, the total probabilities of attaining various performance levels in the longitudinal direction decrease with the decrease in the apparent wave propagation velocity. In other words, considering the uniform excitation scenario increases the probability of attaining various performance levels (including collapse) when compared to other adopted wave propagation velocities scenarios. On the other side, the transverse direction analysis is resulting in a different behavior when adopting different wave propagation velocities. The total probabilities of attaining a performance level or reaching collapse at apparent velocity=200m/sec are the largest (λ for reaching collapse $1.03\text{x}10^{-4}$ at v=200m/sec while $\lambda=7.18\text{x}10^{-5}$ at v=infinity). One could instead express the same information by reporting $1/\lambda$ which gives the return period for exceeding certain performance level (Return period for reaching collapse at v=200m/sec is $1/1.03\text{x}10^{-4} \approx 9700$ years and is $1/7.18\text{x}10^{-5} \approx 14000$ years at uniform excitation scenario). This means that considering the wave passage effect in the bridge transverse direction in this case results in increasing the probability of collapse (or of reaching certain performance level) by a factor of 1.5 relative to the uniform excitation scenario which may be considered a significant jump.

5 SPATIALLY VARIABLE SEISMIC GROUND MOTIONS

The current section is dedicated to study the effect of spatial variability of induced ground motions on the seismic performance and vulnerability of the case study continuous bridge. As will be mentioned later, various parameters affecting the severity of the spatial variability in the seismic ground motions are investigated in the current research work.

5.1 Adopted model for spatial variability in the ground motions

Spatial variability can be described in terms of the cross-power spectral density function between two stations [3] which is given by:

$$S_r(r,\omega) = S_l(\omega)\,.\,R(r,\omega)\,.\exp(i.\omega.\frac{r_v}{v}) \qquad (2)$$

Where,
$S_r(r,\omega)$: Cross-spectrum of a stationary homogenous random ground motions between any two stations
ω: Circular vibration frequency
$S_l(\omega)$: Local in-variant auto-spectrum function; the adopted auto-spectrum function is the modified Kanai-Tajimi spectrum with S_o = 0.01 m^2/sec^3as per Clough and Penzien (1975) [14]. Other parameters which describe the two filters of this spectrum model are listed in table 5.
R(r,ω): Frequency-dependent coherency function, assumed in the form given in Equation 3.
r_v: Separation distance between the two concerned stations projected into the dominant travelling wave direction
v: Apparent travelling wave velocity

It is useful to introduce the following non-dimensional function called coherency function. The shown coherency function in Equation 3 is the adopted one in our model (refer to [11] for all relevant specific details and definitions):

$$R(r,\omega) = \gamma_{ij}(\omega) = \frac{S_{ij}(\omega)}{\sqrt{S_{ii}(\grave{u}).S_{jj}(\grave{u})}} = \exp(-c(\frac{\grave{u}r}{v})) \qquad (3)$$

Where,
c: Loss of coherency parameter
c/v: Ratio between the loss of coherency parameter and the apparent velocity. This ratio usually ranges from 0.0033 to zero. It is basically the inverse of v/c ratio (also referred to by v/α in the literature) ranging from 300m/sec to ∞ [17].

Table 5: Soil filter parameters adopted in the artificially simulated ground motions (refer to [3, 4 & 11] for definitions of all parameters)

Spectrum Type	Soil Type	ω_g (rad/sec)	ζ_g	ω_f (rad/sec)	ζ_f
Type "1"	Soft	2π	0.4	0.2π	0.4
Type "2"	Medium	5π	0.6	0.5π	0.6
Type "3"	Firm	10π	0.8	π	0.8

A simple approach to introduce non-stationary characteristics to the generated stationary motions is through their multiplication by an intensity modulating (envelope) function I(t), commonly referred to as amplitude modulating function. A large number of such intensity modulating functions has been introduced since the 1960's. The adopted function in the current research work is the piecewise-continuous function given by Equation 4 [18]:

$$I(t) = \begin{cases} I_o \left(\frac{t}{t_1}\right)^2 & t \le t_1 \\ I_o & t_1 \ge t \ge t_2 \\ I_o e^{-b(t-t_2)} & t \ge t_2 \end{cases} \quad (4)$$

5.2 Results under spatially variable ground motions

Results of the non-linear analyses considering the spatial variability in the seismic ground motions are presented in tables 6 and 7 in addition to figures 8 and 9. The total probabilities of attaining various performance levels in both bridge directions (longitudinal and transverse) are presented.

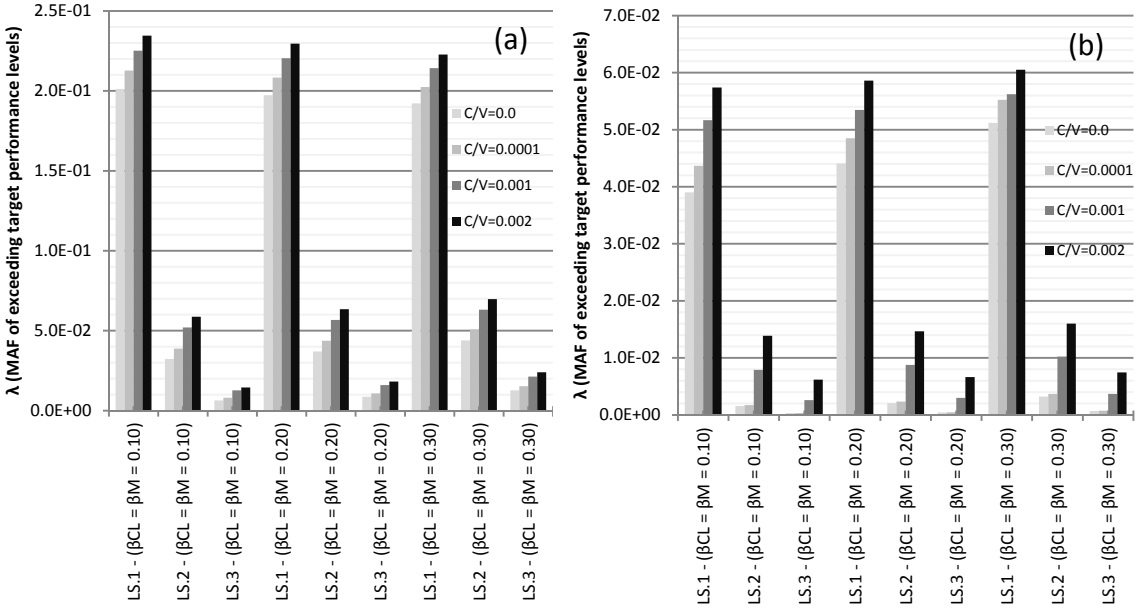

Figure 8: Total probability curves of exceeding various performance levels at different levels of uncertainty in the bridge longitudinal direction for response spectrum type-1 (figure a) and response spectrum type-3 (figure b)

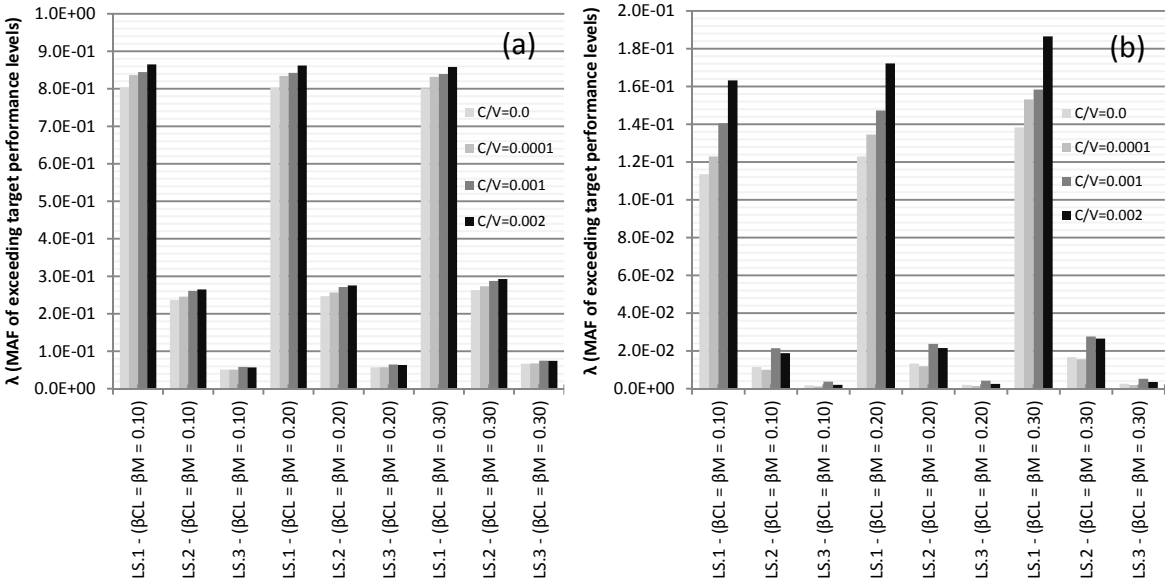

Figure 9: Total probability curves of exceeding various performance levels at different levels of uncertainty in the bridge transverse direction for response spectrum type-1 (figure a) and response spectrum type-3 (figure b)

Table 6: Mean Annual Frequency of exceeding various performance levels for the case study bridge in the longitudinal direction for response spectrum type-1and type-3

Limit State*	c/v	λ (MAF of exceeding target performance levels)					
		Response spectrum type-1			Response spectrum type-3		
		$\beta_{CL}=\beta_M=0.1$	$\beta_{CL}=\beta_M=0.2$	$\beta_{CL}=\beta_M=0.3$	$\beta_{CL}=\beta_M=0.1$	$\beta_{CL}=\beta_M=0.2$	$\beta_{CL}=\beta_M=0.3$
LS-1	0.0000	2.01E-01	1.97E-01	1.92E-01	3.90E-02	4.41E-02	5.12E-02
	0.0001	2.13E-01	2.08E-01	2.02E-01	4.37E-02	4.85E-02	5.52E-02
	0.0010	2.25E-01	2.20E-01	2.14E-01	5.17E-02	5.35E-02	5.62E-02
	0.0020	2.35E-01	2.30E-01	2.23E-01	5.74E-02	5.86E-02	6.05E-02
LS -2	0.0000	3.23E-02	3.70E-02	4.39E-02	1.56E-03	2.07E-03	3.22E-03
	0.0001	3.88E-02	4.38E-02	5.07E-02	1.74E-03	2.35E-03	3.69E-03
	0.0010	5.21E-02	5.67E-02	6.31E-02	7.90E-03	8.76E-03	1.02E-02
	0.0020	5.87E-02	6.34E-02	6.98E-02	1.39E-02	1.47E-02	1.60E-02
LS -3	0.0000	6.37E-03	8.67E-03	1.27E-02	3.32E-04	4.36E-04	6.93E-04
	0.0001	8.06E-03	1.08E-02	1.53E-02	3.35E-04	4.57E-04	7.60E-04
	0.0010	1.27E-02	1.60E-02	2.12E-02	2.60E-03	2.99E-03	3.70E-03
	0.0020	1.45E-02	1.82E-02	2.40E-02	6.18E-03	6.65E-03	7.45E-03

* LS-1=Operational Limit state, LS-2=Life safety and LS-3=Complete Collapse (Refer to table 2 for limit states description)

Table 7: Mean Annual Frequency of exceeding various performance levels for the case study bridge in the transverse direction for response spectrum type-1and type-3

Limit State*	c/v	λ (MAF of exceeding target performance levels)					
		Response spectrum type-1			Response spectrum type-3		
		$\beta_{CL}=\beta_M=0.1$	$\beta_{CL}=\beta_M=0.2$	$\beta_{CL}=\beta_M=0.3$	$\beta_{CL}=\beta_M=0.1$	$\beta_{CL}=\beta_M=0.2$	$\beta_{CL}=\beta_M=0.3$
LS-1	0.0000	8.03E-01	8.02E-01	8.01E-01	1.09E-01	1.18E-01	1.33E-01
	0.0001	8.36E-01	8.34E-01	8.32E-01	1.19E-01	1.30E-01	1.48E-01
	0.0010	8.44E-01	8.42E-01	8.39E-01	1.37E-01	1.44E-01	1.55E-01
	0.0020	8.65E-01	8.62E-01	8.58E-01	1.61E-01	1.69E-01	1.83E-01
LS -2	0.0000	2.37E-01	2.47E-01	2.63E-01	1.15E-02	1.31E-02	1.63E-02
	0.0001	2.46E-01	2.57E-01	2.74E-01	9.96E-03	1.18E-02	1.53E-02
	0.0010	2.61E-01	2.71E-01	2.87E-01	2.13E-02	2.35E-02	2.73E-02
	0.0020	2.65E-01	2.76E-01	2.92E-01	1.88E-02	2.15E-02	2.63E-02
LS -3	0.0000	5.09E-02	5.68E-02	6.66E-02	1.82E-03	2.09E-03	2.65E-03
	0.0001	5.11E-02	5.72E-02	6.76E-02	1.27E-03	1.52E-03	2.03E-03
	0.0010	5.81E-02	6.45E-02	7.50E-02	3.81E-03	4.33E-03	5.31E-03
	0.0020	5.70E-02	6.35E-02	7.45E-02	2.11E-03	2.62E-03	3.62E-03

* LS-1=Operational Limit state, LS-2=Life safety and LS-3=Complete Collapse (Refer to table 2 for limit states description)

As shown in figures 8 and 9 in addition to tables 6 and 7, the total probabilities of attaining various performance levels in both bridge directions (longitudinal and transverse) increase due to spatial variability of ground motions for the different loss of coherency degrees. This means that when the degree of the loss of coherency increases the probability of attaining various performance levels including collapse limit state increases accordingly. Moreover, considering the uncertainties in demand, capacity and in modeling results also in increasing the probability of attaining various performance levels including collapse. For example, the total probability of attaining a performance level (or even reaching collapse) at c/v = 0.002 is the largest (λ for reaching collapse is $1.45\text{x}10^{-2}$ at c/v=0.002 while $\lambda=6.37\text{x}10^{-3}$ at c/v=0.0 in the longitudinal direction for $\beta_{CL}=\beta_M=0.1$). This means that accounting for the spatial variability of the ground motions generally results in increasing the total probability of reaching collapse for this specific example to 2.3 times its value for the uniform excitation scenario. Similar results are obtained in the bridge transverse direction as shown clearly in figure 9. Also, considering the uncertainties in demand, capacity and modeling alters the results and increases the total probability of attaining a certain performance level by a factor of 1.3 on average.

Finally, considering the response spectrum type 1 (soft soil) results in a significant increase in the total probability of attaining a performance level (or reaching collapse) relative to other harder soil types. For example, λ associated with reaching collapse limit state equals $1.45\text{x}10^{-2}$ for response spectrum type 1 (soft soil) while λ equals $6.18\text{x}10^{-3}$ for response spectrum type 3 (firm soil) at c/v=0.002 in the longitu-

dinal direction at $\beta_{CL}=\beta_M=0.1$, which means that the probability of collapse in soft soil may be 2.4 times that in case of firm soil.

6 CONCLUSIONS

A few conclusions that could be drawn from the presented research are:

1- Considering uncertainties in the demand, capacity and modeling may significantly affect the vulnerability analyses results as it could occasionally underestimate the mean annual frequency of reaching collapse if such uncertainties are inaccurately assumed. For instance, an underestimation in the order of about 60% in the mean annual frequency of reaching collapse is reported herein for the case of a travelling apparent wave velocity, v=400m/sec, in the transverse direction of the case study bridge if uncertainties in capacity, β_{CL}, and modeling, β_M, are inaccurately considered as 0.1 instead of 0.3 in the vulnerability analysis.

2- The bridge transverse direction is more sensitive to the difference in the arrival time of the seismic records at different supports than the longitudinal direction due to the bridge relatively smaller out-of-plane stiffness compared to its longitudinal direction in which the deck acts as a rigid diaphragm.

3- The wave passage effect depends on the frequency content of the adopted seismic record. As the frequency content in the seismic record increases, the effect of the difference in the wave's arrival time accordingly increases.

4- Considering the spatial variability in the seismic ground motions results in increasing the total probability of attaining a performance level or reaching collapse relative to the uniform excitation scenario. Besides, increasing the degree of loss in coherency between the induced ground motions increases the probability of attaining a performance level or reaching collapse accordingly.

5- The soft soil profiles result in increasing the bridge sensitivity and vulnerability to the spatial variability in the seismic ground motions compared to firm soil types.

ACKNOWLEDGEMENT

The research reported here was supported by the European Union Project PIRSES-GA-2010-269222: Analysis and Design of Earthquake Resistant Structures (ADERS) of the FP7-PEOPLE-2010-IRSES, Marie Curie Actions. This support is gratefully acknowledged by the authors.

REFERENCES

[1] Abrahamson, N.A., Schneider, J.F. and Stepp, J.C. (1991). "Empirical spatial coherency functions for application to soil-structure interaction analyses". Earthquake Spectra, Vol.7 (2) pp. 1-27.

[2] Open System for Earthquake Engineering Simulation (Opensees) (2009). Pacific Earthquake Engineering Research Centre, University of California, Berkeley, http://opensees.berkeley.edu/.

[3] Ramadan, O.M.O. and Novak, M. (1994). "Simulation of multi-dimensional, anisotropic ground motions," J. engrg. mech., ASCE, Vol. 120, No 8, pp 1773-1785.

[4] Ramadan, O.M.O. and Novak, M. (1993). "On the simulation of spatially incoherent random ground motions," J. engrg. mech., ASCE, Vol. 119, No. 5, pp 997-1016.

[5] Liao, S. (2006) "Physical Characterization of Seismic Ground Motion Spatial Variation and Conditional Simulation for Performance-Based Design" Ph.D. thesis, Drexel University.

[6] Medina, R. (2002) "Seismic Demands for non-deteriorating frame structures and their dependence on ground motions". Ph.D. thesis, Stanford University.

[7] Taylor, E. (2007)." The Development of Fragility Relationships for Controlled Structures". Master of Science thesis, Washington University.

[8] ECP 201 (2008) "Egyptian Code of Practice no. 201 for Determination of Loads and Forces for the Structural and Civil Works", Research Centre for Housing and Construction, Ministry of Housing, Utilities and Urban Planning, Cairo, Egypt. Final Draft 2009.

[9] Haselton, C.B. (2006),"Assessing Seismic Collapse Safety of Modern Reinforced Concrete Moment Frame Buildings". Ph.D. thesis, Stanford University.

[10] Seismic design manual (2000), Structural Engineering Association of California.

[11] Elhowary, H.A. (2014) "A Probabilistic framework for assessing seismic performance of concrete bridges subjected to spatial variable seismic ground motions" (2014). Ph.D. thesis, Cairo University, to be published.

[12] Monti, G., Nuti, C, and Pinto, P.E. (1996). "Nonlinear Response of Bridges UnderMultisupport Excitation."Journal of Structural Engineering, ASCE, Vol. 122 (No. 10).

[13] Tzanetos, N., Elnashai, A.S., Hamdan, F, Antoniou, S. (1998). "Inelastic Dynamic Response of RC Bridges to Non-Synchronous Earthquakes Input Motion" ESEE Research Report No.98-6, Civil Engineering Department, Imperial College, London, UK.

[14] Clough, R.W., and Penzien, J. (1993). Dynamics of structures, 2nd Ed., McGraw-Hill, New York.

[15] Wang, J., Athol, C., Nigel, C., and Peter, M. (2004). "Inelastic Responses of Long Bridges to Asynchronous Seismic Inputs", 13th World Conference on Earthquake Engineering.

[16] Elhowary, H.A. and Mehanny, S.S.F. (2011), "Seismic Vulnerability Evaluation of RC Moment Frame Buildings in Moderate Seismic Zones," Earthquake Engineering and Structural Dynamics, Vol. 40, Issue 2, pp. 215-235.

[17] Zerva, A. (2009) Spatial Variation of Seismic Ground Motions: Modelling and Engineering Applications (Advances in Engineering Series). Ed. Haym Beranoya. CRC Press, Taylor & Francis Group, FL.

[18] Zerva, A. (1992). "Seismic ground motion simulations from a class of spatial variability models." Earthquake Engineering and Structural Dynamics, 21, 351–361.